Finite-size effects in the dynamics of glass-forming liquids

Ludovic Berthier,[1] Giulio Biroli,[2] Daniele Coslovich,[1] Walter Kob,[1] and Cristina Toninelli[3]
[1]*Laboratoire Charles Coulomb, UMR 5221, CNRS and Université Montpellier 2, Montpellier, France*
[2]*Institut de Physique Théorique (IPhT), CEA, and CNRS URA 2306, 91191 Gif-sur-Yvette, France*
[3]*Laboratoire de probabilités et modèles aléatoires, UMR CNRS 7599, Université Pierre et Marie Curie et Université Denis Diderot, 4 Place Jussieu, 75252 Paris Cedex 05, France*
(Received 16 March 2012; published 10 September 2012)

We present a comprehensive theoretical study of finite-size effects in the relaxation dynamics of glass-forming liquids. Our analysis is motivated by recent theoretical progress regarding the understanding of relevant correlation length scales in liquids approaching the glass transition. We obtain predictions both from general theoretical arguments and from a variety of specific perspectives: mode-coupling theory, kinetically constrained and defect models, and random first-order transition theory. In the last approach, we predict in particular a nonmonotonic evolution of finite-size effects across the mode-coupling crossover due to the competition between mode-coupling and activated relaxation. We study the role of competing relaxation mechanisms in giving rise to nonmonotonic finite-size effects by devising a kinetically constrained model where the proximity to the mode-coupling singularity can be continuously tuned by changing the lattice topology. We use our theoretical findings to interpret the results of extensive molecular dynamics studies of four model liquids with distinct structures and kinetic fragilities. While the less fragile model only displays modest finite-size effects, we find a more significant size dependence evolving with temperature for more fragile models, such as Lennard-Jones particles and soft spheres. Finally, for a binary mixture of harmonic spheres we observe the predicted nonmonotonic temperature evolution of finite-size effects near the fitted mode-coupling singularity, suggesting that the crossover from mode-coupling to activated dynamics is more pronounced for this model. Finally, we discuss the close connection between our results and the recent report of a nonmonotonic temperature evolution of a dynamic length scale near the mode-coupling crossover in harmonic spheres.

DOI: 10.1103/PhysRevE.86.031502 PACS number(s): 64.70.Q−, 64.70.kj, 05.20.Jj, 05.10.−a

I. INTRODUCTION

Theoretical studies of the glass transition make heavy use of computer simulations of both simple model systems such as lattice glass models or kinetically constrained spin models and more realistic models of liquids studied through molecular dynamics simulations [1]. Usually, numerical studies are performed with periodic boundary conditions using system sizes that are "large enough" to provide results that are representative of the thermodynamic limit [2]. From this point of view the existence of finite-size effects is a nuisance. However, as discovered in the context of standard critical phenomena [3], a thorough study of finite-size effects can be very informative: It allows one to measure the growing correlation lengths, to ascertain the critical properties, to obtain quantitative information about fluctuations of the order parameter, and to provide crucial tests for theoretical approaches. While a large amount of work has been devoted to measuring the spatial extent of growing correlation length scales [4] in supercooled liquids, only a few studies have paid specific attention to finite-size effects [5–12], while an even smaller number of studies have made explicit use of finite-size scaling techniques to explore glass transitions [13–16]. The aim of this paper is to fill this gap and to address from a theoretical point of view the issue of finite-size scaling in supercooled liquids.

For quite a long time, the glass transition was considered a puzzling phenomenon, corresponding to an obvious change between fluid and solid states, but without any of the signs found near standard phase transitions, apart from a dramatic but gradual viscosity increase when approaching the experimental glass temperature [17,18]. In apparent agreement with this situation, early numerical simulations did not reveal the strong system size dependencies that would for instance smear out singular behaviors expected near ordinary phase transitions [19,20]. In more recent years, important progress has been made regarding the status of the glassy state and of the relevant length scales characterizing systems approaching the glass transition [21]. In particular, two decades of active research on dynamic heterogeneity in amorphous materials have established that the formation of rigid amorphous structures is indeed accompanied by nontrivial spatiotemporal fluctuations, which become more pronounced upon approaching the glassy phase and are characterized by growing dynamic correlation length scales [4].

A more recent line of research aims at demonstrating also the existence of growing static correlation length scales, using point-to-set correlation functions [22–27]. The idea is to confine the system using carefully chosen amorphous boundary conditions to detect the existence of multipoint static correlations in viscous liquids. The point-to-set length scale quantifies the spatial extent of these correlations. However, it is still unclear whether such static length scales are equivalent to [28], indirectly related to [29], or even decoupled from [30–33] dynamic ones. Actually, the answer to this question may also depend on the level of supercooling, thus revealing the existence of physically distinct temperature regimes.

As is well known in computational studies of phase transitions, the size of the system can be used as an additional physical length scale in the problem. Thus, the interplay between the system size and the correlation lengths can be used to

probe the role played by dynamic and static correlation lengths in determining the physical behavior of supercooled liquids. In particular, an important motivation for the present work is the recent numerical finding [31] that, for a system of harmonic spheres, a surprising nonmonotonic temperature evolution of dynamic correlation length scales near an amorphous wall has been detected in the temperature regime corresponding to the mode-coupling temperature [34], which was interpreted as direct evidence that the physical mechanisms for relaxation are different at moderate and low temperatures. If true, this interpretation suggests that a similar change of behavior could also occur in the bulk and could be revealed by studying carefully finite-size effects in the same temperature regime. We shall see below that our data indeed support the hypothesis of Ref. [31], at least for the harmonic sphere system.

As mentioned above, finite-size effects can also be used to test and compare theoretical approaches. Indeed, these provide different, and sometimes contrasting, predictions on the nature and extent of correlation lengths and fluctuations in viscous liquids [21]. For instance, kinetically constrained models [35] and the dynamic facilitation approach [36] focus on dynamic length scales that usually diverge at a zero-temperature dynamic critical point [37], and random first-order transition theory [38,39] predicts the occurrence of a narrowly avoided mode-coupling dynamic singularity in the moderately supercooled regime, with a crossover toward a second regime controlled by a thermodynamic singularity and activated dynamics at lower temperatures, each domain being associated with its own diverging length scale [40]. As a consequence, the interplay between correlation lengths and system size and, hence, the resulting finite-size effects depend on the theoretical approach. A central motivation for the present work is to obtain, discuss, and compare to numerical simulations the theoretical predictions concerning finite-size effects.

We emphasize that since our focus is on highly viscous supercooled liquids, we do not discuss the literature about finite-size effects in simple liquids, which is a different topic, for which hydrodynamic effects, ignored here, play a more central role [41,42].

In summary, this paper presents a comprehensive theoretical study of finite-size effects in supercooled liquids. Our aim is to provide useful practical information about the relevance of finite-size effects in computer studies of the glass formation, test theoretical approaches, and also obtain new insights about the nature of the fluctuations revealed by finite-size studies, in particular in the region of the mode-coupling crossover.

The paper is organized as follows. In Sec. II we provide general theoretical arguments that are relevant for the description confined supercooled liquids. In Sec. III, we use specific theoretical approaches to make predictions regarding finite-size effects. In Sec. IV we introduce a new lattice glass model with an avoided mode-coupling singularity whose strength can be tuned by changing the lattice topology and use it to study finite-size effects. In Sec. V we provide molecular dynamics simulations of four model liquids with distinct structures and kinetic fragilities. In Sec. VI we close the paper with a discussion of the results. More details about the new lattice glass model introduced in Sec. IV are given in the Appendix.

II. EMERGENCE OF FINITE-SIZE EFFECTS IN FRAGILE LIQUIDS

The relaxation time of glass-forming materials approaching the glass transition can be described by the thermally activated form

$$\tau_\alpha \approx \tau_0 \exp\left[\frac{E(T)}{T}\right], \tag{1}$$

where the activation energy $E(T)$ increases when temperature decreases for fragile materials, whereas it is constant for strong glass-formers [21]. Here and in the following we shall absorb the Boltzmann constant k_B in the definition of T. The temperature dependence of $E(T)$ in Eq. (1) means that the nature of the relaxing "entities," whatever they are, changes with temperature. A growing activation energy actually suggests an increasing cooperativity in the relaxation events, corresponding to the correlated motion of an increasing number of particles. Thus, by reducing the system size one expects, all other things being equal, that the dynamics starts to differ from bulk behavior when the linear size becomes comparable to the size of these correlated regions. Thus, it is natural to expect the emergence of a characteristic length scale, which we denote by $\ell_{\rm FS}(T)$ in the following, characterizing finite-size effects such that bulk relaxation is obtained when the system size is larger than $\ell_{\rm FS}(T)$. In cases where the dynamics is characterized by several length scales, the behavior of $\ell_{\rm FS}(T)$ will be more complicated, as we shall see. In any case, we believe that finite-size studies should provide a new way to probe dynamical correlations and cooperativity in glass-forming liquids [15].

By using a very general argument, one can show that $\ell_{\rm FS}(T)$ must grow for fragile liquids when temperature decreases. The starting point of our argument is to recall that an upper bound for the relaxation time scale for a system of linear size L can be obtained by assuming the worst-case scenario, namely that all particles have to move together in a cooperative way to relax the structure. This leads to an upper bound for $\tau_\alpha(L,T)$ that scales with L as

$$\tau_\alpha(L,T) \leqslant \tau_{ub}(L,T) = \tau_0 \exp\left(\frac{cL^d}{T}\right), \tag{2}$$

where τ_0 is a microscopic time scale, c is a numerical constant, and d is the spatial dimension. Note that for systems evolving with stochastic dynamics and with discrete degrees of freedom this is a rigorous statement [43]. For other systems, this result is expected on general grounds but a rigorous proof is probably out of reach.

Now, consider an infinite system characterized by the relaxation time scale $\tau_\alpha(T) = \tau_\alpha(L \to \infty, T)$, and then decrease its size while simultaneously measuring $\tau_\alpha(L,T)$. By definition, the structural relaxation time will not change until $\ell_{\rm FS}(T)$ is reached. A lower bound for this length can be obtained by noticing that a constant $\tau_\alpha(L,T)$ as a function of L would necessarily violate the bound in Eq. (2) at small L and large enough $\tau_\alpha(T)$. Thus, dynamical finite-size effects must appear when (or before) $\tau_\alpha(\infty,T)$ becomes equal to $\tau_{ub}(\ell_{\rm FS},T)$. Therefore, we find

$$\ell_{\rm FS}(T) \geqslant \left(\frac{T}{c}\ln\left[\frac{\tau_\alpha(T)}{\tau_0}\right]\right)^{1/d}. \tag{3}$$

By using Eq. (1), this result implies that, up to a proportionality constant, $\ell_{\rm FS}(T)$ must increase with temperature at least as $E(T)^{1/d}$. Note that this result does not imply anything about the precise dependence of τ_α on L, in particular whether or not this dependence is monotonic. However, it shows that for fragile liquids the length obtained by dynamical finite-size effects studies has to increase when temperature decreases. This growth would be faster than $(1/T)^{1/d}$ or $[T/(T-T_{VFT})]^{1/d}$, in the respective cases where $\tau_\alpha(T)$ follows a Bässler or a Vogel-Fulcher temperature dependence.

At this point, three important remarks are in order.

(1) The lower bound on $\ell_{\rm FS}(T)$ only becomes meaningful when $\{T\ln[\tau_\alpha(T)/\tau_0]/c\}^{1/d} \geqslant a$, where a is the typical interparticle distance. The temperature at which this takes place of course depends on the values of the constant c and of τ_0 and may actually correspond to very deep supercooling, i.e., very large values of τ_α. It would be interesting to have an estimate of c and τ_0 for a given liquid to understand what is the highest temperature at which our argument becomes useful.

(2) For a strong (i.e., Arrhenius) liquid, $E(T)=E$, one finds that $\{T\ln[\tau_\alpha(T)/\tau_0]/c\}^{1/d}$ does not depend on temperature. This makes perfect sense within the physical picture where strong liquids relax by localized and independent thermally activated events. In this case $\ell_{\rm FS}$ should be temperature independent and roughly equal or at least proportional to the microscopic length scale a.

(3) The lower bound we obtained for $\ell_{\rm FS}(T)$ actually coincides with the one obtained in Ref. [23] for the static point-to-set length. This is reasonable because one expects the dynamical length probed by finite-size effects to be larger than (or equal to) the static point-to-set length.

III. SPECIFIC THEORETICAL PREDICTIONS

Having argued by general arguments that $\ell_{\rm FS}(T)$ increases when T decreases for fragile liquids and hence should be related to cooperative relaxation of some sort, we now address the precise form of $\tau_\alpha(L,T)$ as a function of L and the possible physical mechanisms behind the increase of $\ell_{\rm FS}(T)$. Since this partially depends on the particular theoretical description used, we consider several different cases.

An important conclusion of the following sections is that $\ell_{\rm FS}(T)$ cannot be univocally related to one of the several correlation lengths introduced recently. This relation depends on the theory: $\ell_{\rm FS}(T)$ may coincide with a static correlation, like the point-to-set one, or coincide with the dynamic correlation length, or be only indirectly related to either one of them.

A. Cooperatively rearranging regions

There are several theories that explain the relaxation process in supercooled liquids in terms of cooperative rearrangements of regions involving a growing number of particles. Theories falling in this category are the Adam-Gibbs theory [44], the frustration-limited domain approach [45,46], and random first-order transition (RFOT) theory [38,39,47]. For RFOT theory, a different dynamical process described by mode-coupling theory (MCT) [34] is responsible for relaxation for temperatures higher than $T_{\rm MCT}$, and this regime is discussed separately below in Sec. III C.

In all these theories the relaxation time is derived by assuming activated dynamic scaling and using as a characteristic length scale the linear size of the rearranging regions. Thus, the logarithm of the relaxation time scale is proportional to the length scale raised to some power, which for instance is equal to d in the Adam-Gibbs case [44]. The physical mechanism responsible for the growth of this length scale and the exponent of the power law depend on the details of the theory.

By assuming that cooperative relaxation events are uncorrelated, as is usually done, the primary effect of decreasing system size is to decrease the value of the activation energy from its bulk value, because the number of particles involved decreases, once the system size becomes smaller than the typical size of a rearranging region. Thus, for all these theories, one expects $\tau_\alpha(L,T)$ to be a monotonically increasing function of L approaching the bulk value from below for L of the order of the size of the rearranging regions. This is directly reminiscent of finite-size effects near a second-order phase transition [3], where divergences are smeared out by finite system sizes. The only peculiarity of the glass transition would be the occurrence of activated, rather than algebraic, forms of dynamic scaling. It would be interesting to know whether some kind of scaling formula holds for $\tau_\alpha(L,T)$ [or $\log\tau_\alpha(L,T)$].

This behavior of $\tau_\alpha(L,T)$ as a function of L is also similar to the one expected within RFOT theory using amorphous boundary conditions [21,28]. However, the physical mechanisms conjectured to play a role for small L are different from the periodic boundary conditions considered here. In the former, the dynamics accelerates because the boundary condition lowers the free energy of a single state. Therefore relaxation occurs inside this state and is hence faster than in the activated regime in which the other states should also be visited. With periodic boundary conditions instead, the dynamics is activated but the barrier decreases if L becomes smaller.

B. Defect models

Defect models [35], and in particular dynamical facilitation models [36], have been widely used to study dynamical heterogeneities and spatial correlations in viscous liquids, but dynamical finite-size effects have not been specifically discussed.

In defect models, whether cooperative or not [35], there are at least two relevant length scales. One is the typical distance between defects, $\xi_d \propto c^{-1/d}$ (where c is the defect density), and the other is related to the size of dynamical correlations. The two are not necessarily equal, and the latter can possibly be much larger than the former depending of the model and the dimensionality [48]. Assuming that the equilibrium concentration of defects is unaffected by confinement, we expect ξ_d to be the most relevant length scale for the finite-size effects. In fact, for intermediate system sizes (i.e., for L between ξ_d and the dynamic correlation length), one might expect that $\tau(L,T)$ deviates only weakly from its bulk value, as the nature of dynamical facilitation remains essentially unaffected. This statement is straightforward for diffusing defects and noncooperative constrained models, but it has to be taken with some caution for cooperative models which have a more complicated dynamics typically characterized by several (and possibly a hierarchy of) dynamic length scales [6,35].

By contrast, the nature of the dynamical processes must change qualitatively when L competes with ξ_d. Indeed, for $L \simeq \xi_d$ about half of the equilibrium configurations contain strictly no defect. In this case, the system has to either use a different channel for relaxation or create a new defect and then relax by defect diffusion. (Note that this second scenario is strictly forbidden in spin-facilitated models, which thus become instead nonergodic in this limit [35].) In both cases the corresponding relaxation time is expected to be larger than the one for configurations having a defect from the beginning, which instead relax on a time scale of the order of the bulk relaxation time. Therefore, the average relaxation time is expected to start to increase strongly when $L \simeq \xi_d$ (and to become infinite in constrained spin models). The behavior for $L < \xi_d$ is less clear because in this case the system typically does not have any defect in equilibrium configurations and, hence, relaxes in a way different from the one used for $L \gg \xi_d$, and no alternative relaxation channel is described within the defect approach. Since in this case the shape of $\tau_\alpha(L,T)$ is determined by the L dependence of this unknown relaxation mechanism we cannot say much about it. However, using the general argument developed above we know that for fragile liquids $\tau_\alpha(L,T)$ has to decrease when the system size is reduced below $\{T \ln[\tau_\alpha(T)/\tau_0]/c\}^{1/d}$. Thus, in the case of fragile liquids and within the framework of defect diffusion theories we expect $\tau_\alpha(L,T)$ to have a nonmonotonic behavior that can be more or less pronounced depending on the underlying model. Instead, in the case of Arrhenius liquids, it is possible that $\tau_\alpha(L,T)$ increases with decreasing L until the linear system size is almost of the order of the interparticle distance.

As final comments, we first stress that some form of facilitation dynamics could additionally be introduced within the theories of cooperative rearranging regions. Thus some mild nonmonotonic behavior can be present even in that case. Second, whatever is the correct theory, there could be actually several length scales playing a role. It is likely that larger length scales are affected first by the confinement such that very large domains disappear first when L is reduced, which should somehow truncate the distribution of relaxation times, making the average (e.g., the first moment of the distribution) smaller. This suggests that finite-size effects could manifest themselves at very long times only, which could correspondingly only affect the tail of time correlation functions.

C. The mode-coupling theory crossover

In the framework of the mode-coupling theory of the glass transition [34], a dynamical transition accompanied by a diverging dynamic correlation length scale [49] takes place at a finite temperature $T_{\rm MCT}$. It is well known that the transition predicted by the theory actually does not take place in finite-dimensional models and in experiments. Instead, it is replaced by a crossover occurring near the temperature extracted from fitting the dynamical relaxation to scaling predictions of the theory, although the precise nature of this crossover is not well understood [39,50]. RFOT theory naturally includes mode-coupling theory, but at present it cannot describe the nature of the crossover from mode-coupling to activated relaxation in much detail [39]. Decreasing L at constant temperature above $T_{\rm MCT}$ (and, of course, below the onset temperature), we again expect a nonmonotonic size dependence of $\tau_\alpha(L,T)$ due to the competition between two effects, which we now explain.

When considered from the point of view of random first-order transitions [39], a physical interpretation of the dynamics within the mode-coupling regime is that relaxation occurs along unstable modes that become less and less unstable and more collective upon approaching $T_{\rm MCT}$, thus leading to diverging dynamic correlations [49]. By reducing the system size below the dynamic correlation length, these unstable extended modes are the most easily affected, and confinement should render some of these modes stable, thus closing some relaxation channels. The effect would then be to slow down relaxation, or equivalently to shift the apparent value of $T_{\rm MCT}$ to larger temperature [40,51].

However, decreasing the system size has a second consequence. The singularity predicted by the theory cannot occur in a finite-size system, and therefore $\tau_\alpha(L,T)$ cannot increase indefinitely by decreasing L. In fact this growth is bounded from above by the general argument detailed in Sec. II even though this may happen on quite a small length scale. Within RFOT theory, the increase of $\tau_\alpha(L,T)$ at small L should be cut off for length scales such that relaxing via the mode-coupling channel becomes slower than the activation channel. Then, for even smaller L, relaxation will proceed by cooperative rearrangements (as it does in the bulk below $T_{\rm MCT}$) and this should lead, as in Sec. III A, to a decrease of $\tau_\alpha(L,T)$ by decreasing L.

Overall, we should then observe a nonmonotonic behavior of the relaxation time in the mode-coupling regime, because using systems with finite sizes has a qualitatively different impact on mode-coupling dynamics (which slows down in confinement) and activated dynamics (which accelerates in confinement).

Although already quite complex, the picture depicted above is certainly still too simplistic. As stated before, the mode-coupling crossover is not well understood and it is thus likely that dynamical finite-size effects will turn out to be quite subtle and lead to a very complex behavior, as found in seemingly simpler mean-field models [52–54]. In order to shed some more light on this crossover, we consider in the following a finite-dimensional model that displays an avoided mode-coupling singularity.

IV. A LATTICE GLASS MODEL WITH AN AVOIDED MODE-COUPLING TRANSITION

A. Kac-Fredrickson-Andersen model

We study a two-dimensional Kac version of the spin-facilitated model extensively studied by Fredrickson and Andersen (FA) [55–57], which we call the Kac-Fredrickson-Andersen (KFA) model. This is defined by a noninteracting Hamiltonian

$$H = \sum_i n_i, \tag{4}$$

where $n_i = 0,1$ represents a binary mobility defect variable. The average density of spins in the excited state is $c(T) = [1 + \exp(1/T)]^{-1}$. For the dynamics, we choose the two-spin facilitation rule, as in the original model [55]: To be able to flip, a spin must possess at least two neighbors which are both in the excited state $n_i = 1$.

A generalization to a Kac version of the model can be obtained by introducing a new geometrical parameter, K, which characterizes the range of the spin connectivity within a regular two-dimensional square lattice. In the standard FA model in two dimensions, the spin at position $\mathbf{r}$ has four nearest neighbors that contribute to facilitating its dynamics. They occupy the positions $\mathbf{r}+\mathbf{e_x}$, $\mathbf{r}-\mathbf{e_x}$, $\mathbf{r}+\mathbf{e_y}$, and $\mathbf{r}-\mathbf{e_y}$, where $\mathbf{e_x}$ and $\mathbf{e_y}$ are unit vectors along the horizontal and vertical directions, respectively. In our Kac-version, the spin at position $\mathbf{r}$ remains facilitated by four "neighbors," which are now located at positions $\mathbf{r}+i\mathbf{e_x}$, $\mathbf{r}-j\mathbf{e_x}$, $\mathbf{r}+k\mathbf{e_y}$, and $\mathbf{r}-l\mathbf{e_y}$, where (i,j,k,l) are four random numbers chosen in the set $\{1,\ldots,K\}$ according to a procedure that will be detailed below. Thus, the KFA model contains quenched disorder, and spins can interact on the lattice over a range K that can be tuned at will and be made arbitrarily large, while keeping the spin connectivity constant and equal to that of the original $K=1$ model.

To generate an instance of the lattice, we start from the leftmost site of a given line and connect it at random to one of its K right neighbors. We then move to the right by one lattice spacing and connect the new site at random to one of its K right neighbors, excluding the one that has been connected at the previous step. This procedure is then iterated up to the $(K-1)$-th site of the line always connecting the current site at random to one of its K right neighbors excluding the ones that have been previously connected. In order to guarantee that at the end of the procedure each site has a right and a left neighbor we proceed as follows for the remaining sites. When choosing the right neighbor of site i we first check whether $i+1$ already has a left neighbor. If this is not the case we connect i to $i+1$; otherwise we pick the right neighbor of i uniformly at random among the sites $i+2,\ldots,i+K$ which have not yet been assigned a left neighbor. We then iterate this procedure up to the end of the line imposing periodic boundary conditions. In this way we generate a random one-dimensional lattice with connectivity two at each site and a range equal to K. We then repeat the procedure for each line and column of the square lattice to define an instance of the KFA model. When performing simulations of the KFA model, we also average over independent realizations (typically 2000) of the lattice.

Note that in the limit $K\to\infty$ the probability ϵ that a site is connected to its right nearest neighbor does not decay to zero; however, it can easily be bounded from above by $\exp(-1)$ and the numerics indicates that this probability saturates at a lower value $\epsilon\simeq\exp(-2)$. Thus in the $K\to\infty$ limit, the geometry becomes the one of a Bethe lattice with connectivity equal to four, decorated by loops occurring with probability at most $\epsilon^4\simeq\exp(-8)$ and a finite-temperature singularity occurs. We expect this transition to share important similarities with the mode-coupling transition as is the case on the pure Bethe lattice [58]. In particular, time correlation functions should decay in a two-step manner with power laws characterizing the approach and departure from the intermediate time plateau and an algebraic divergence of the temperature evolution of the equilibrium relaxation time. Instead for $K=1$ the topology of the square lattice is recovered and the physical behavior is that of a cooperative kinetically constrained model, with a divergence of time scales and length scales at $T=0$ only [59].

The crucial point for our purposes is that, for a large but finite K, we expect the dynamics to be controlled in some temperature range by the mode-coupling singularity because the system locally resembles the $K=\infty$ decorated tree, but the singularity must be avoided because the square lattice topology eventually dominates at large enough length scales.

Therefore, as is believed to be the case in finite-dimensional glasses, the mode-coupling singularity is "avoided" when temperature decreases because of the presence of some "activated processes." Actually, in this case it is more correct to call these processes cooperative instead of activated since they are due to the diffusion of macro-vacancies [59]. There are however two important differences between the KFA model and supercooled liquids. First, in the KFA model both temperature regimes and the related physical behaviors are well understood, and thus our model smoothly interpolates between limits that are under control. Second, we can tune the parameter K to be very close or very far from the mode-coupling limit, and thus we can control the relevance of the infinite-range dynamics for the finite-range model, which is not readily realized in liquids. We note that a closely related attempt to control the importance of mean-field behavior has recently been published [60] in the context of off-lattice models of liquids, following an idea similar to ours where the connectivity is kept constant while increasing the range of the interaction between particles.

In the following we present results of extensive Monte Carlo simulations of the above model using periodic boundary conditions and a lattice of linear size L which we vary. We use a continuous-time Monte Carlo algorithm [61] and study a broad range of parameters, changing in particular the Kac range from $K=1$ to $K=24$ (but note that we only consider the regime $K<L/2$). It is important to stress that depending on K and L, especially at small system sizes, some samples may contain a finite fraction of blocked spins, a "backbone," that will never flip. We disregard these configurations and sample only the ones that do not contain blocked backbones. A different choice would be to average over all configurations and estimate the relaxation time as the time decay of the persistence to a nonzero long-time value. We have chosen the first solution, and so we perform a "biased" average over all ergodic configurations, in order not to mix ergodic and nonergodic configurations in a single average. By contrast, no blocked configurations are found when L is large enough and bulk dynamics is studied. Here, L "large enough" means that the relaxation time and the correlation functions no longer depend on L (and the size dependence of these functions is studied in great detail below). Because the Hamiltonian in Eq. (4) is trivial, it is straightforward to generate equilibrium configurations and to study equilibrium relaxation in the absence of any aging effect. The only limitation is that complete relaxation cannot be observed over our finite time window when temperature is too low, a regime which again depends on the value of K and is of course set by our computer resources.

B. Evidence of a mode-coupling crossover for the bulk dynamics

Following previous work [37], we first probe the bulk equilibrium dynamics in the KFA model by measuring the

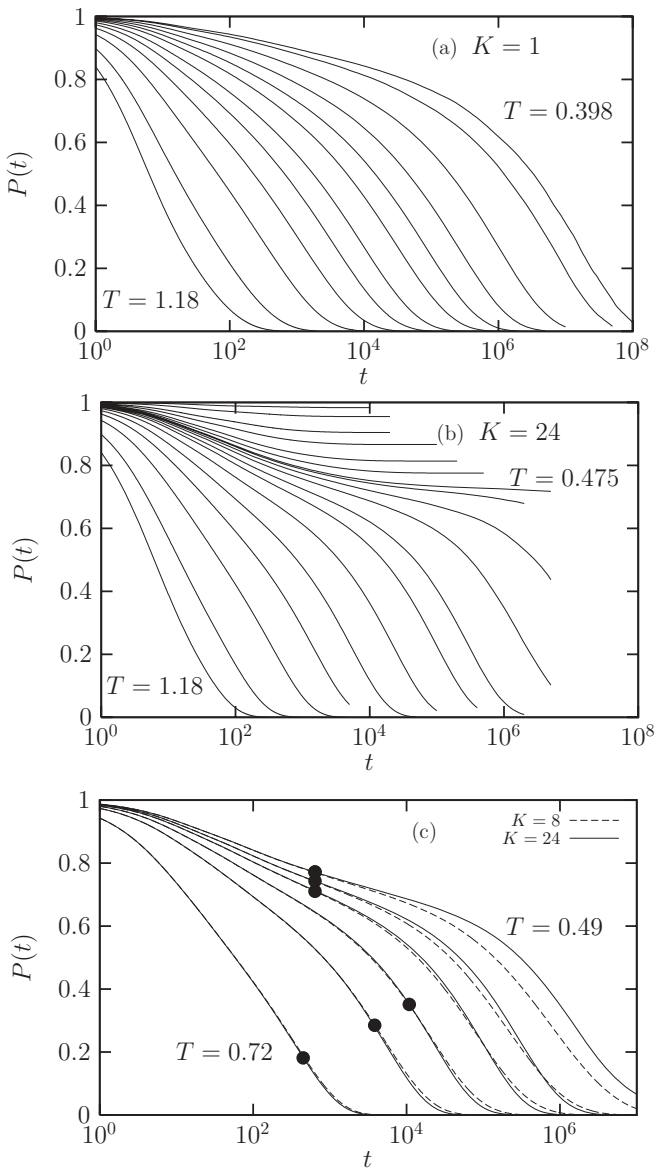

FIG. 1. Time dependence of persistence functions in the KFA model for various connectivity range K and temperatures T. (a) Data for $K = 1$ and decreasing temperatures (from left to right). (b) The data for $K = 24$ and decreasing temperatures (from left to right) clearly show a two-step decay toward an intermediate plateau. (c) Comparison between data for $K = 8$ and $K = 24$ at various temperatures. A filled circle indicates the crossover time scale t^* after which the two sets of data deviate significantly, thus delimiting the (t,T) domain of applicability of mean-field dynamics.

persistence function

$$P(t) = \left\langle \frac{1}{N} \sum_{i=1}^{N} P_i(t) \right\rangle, \tag{5}$$

where $P_i(t) = 1$ if the spin at site i has not changed state between times 0 and t, and $P_i(t) = 0$ otherwise. We have also studied the spin-spin autocorrelation function and have found qualitatively similar results, which are thus not presented here.

Our findings for different connectivity ranges K and temperatures T are presented in Fig. 1. To obtain these data, we have used $L = 150$ for $K = 1$, up to $L = 250$ for $K = 24$, carefully checking the absence of finite-size effects. The data for $K = 1$ in Fig. 1(a) resemble previously published results in cooperative kinetically constrained models [35,37,62–64]. The shape of the persistence function changes very little when temperature decreases. An important point for us is that these curves only display a single decay toward zero instead of the clear two-step decay (termed alpha and beta relaxations) typically found in supercooled liquids. This distinction was often interpreted as being a consequence of working on the lattice because short-time thermal vibrations cannot contribute to relaxation functions [62]. It was later understood that an analog of the beta relaxation could nevertheless appear and be studied in lattice models [50,58,63,64], as we now confirm.

When moving from $K = 1$ to $K = 24$ in Fig. 1(b), which is the largest range studied in this work, we find that the shape of the correlators changes continuously with increasing K. In particular, the short-time dynamics changes from being convex (or quasilogarithmic [62,64]) to becoming concave and converging to an intermediate-time plateau, as can clearly be seen in Fig. 1(b). This two-step decay is also characteristic of the decay of dynamic correlators predicted by mode-coupling theory. Due to the small probability [$\simeq \exp(-8)$] for a site to be in a loop, we expect the system for $K \to \infty$ to be well described by a Bethe lattice for the system sizes which we can numerically explore. We have performed a few simulations directly on the Bethe lattice, as in Ref. [58], and found that, for the range of temperature accessible for $K = 24$, the relaxation functions for $K = 24$ and $K = \infty$ are extremely close, and so we take $K = 24$ as being representative of the infinite-range limit over the accessible temperature range. For the studied connectivity, the transition temperature for the Bethe lattice limit is $T_c = 0.480898$.

Overall, these curves suggest that, as announced, the KFA model crosses over from a mode-coupling-like dynamics at large K toward a dynamics of a different nature at small K, which is cooperative, yielding a super-Arrhenius growth of the relaxation time.

Interestingly, while the data for $K = 1$ appear qualitatively different from the $K = \infty$ counterpart, we find that for intermediate K values, a finite-temperature regime seems to open where the dynamics is qualitatively similar to the mean-field regime, with deviations only appearing at lower temperatures. We confirm these observations in Fig. 1(c), where relaxation data for $K = 8$ and $K = 24$ are superimposed for various temperatures. It is clear that deviations between the two sets of curves are very small at high temperatures and become quite large when T decreases. More precisely, we observe that for each temperature the relaxation data are very similar at short times but differ at long times. This allows the definition of a crossover time scale $t^*(T)$, marked with a closed symbol in Fig. 1(c), such that differences between the two persistence functions only become significant for $t > t^*$. We find that t^* belongs to the alpha relaxation when temperature is not too low, which implies that the correlation functions and thus the relaxation time are controlled, in this temperature regime, by the infinite-range dynamics. However, when temperature is decreased further, t^* now belongs to the beta relaxation. This means that sufficiently close to the dynamic singularity of the $K = \infty$ model, the temperature evolution

of τ_α differs significantly from the infinite-range model, so that the singularity is eventually avoided. Quite remarkably, we also find that the beta relaxation does not seem to be very much affected by this crossover, which could imply that short-time dynamics remains well described by the mean-field limit even at temperatures where the long-time dynamics is already controlled by activated processes. This would suggest that a more precise prescription for the applicability of the mode-coupling predictions should be done in the (time, temperature) domain, rather than by defining a single crossover temperature [39]. In practice, this suggests that mode-coupling theory could still be useful below $T_{\rm MCT}$, at least to describe the short-time dynamics of viscous liquids and estimate for instance the temperature evolution of the Debye-Waller factor [34,65].

A much sharper identification of the crossover is found by studying the alpha-relaxation time of the system. We extract $\tau_\alpha(T)$ from the relaxation curve using the definition $P[\tau_\alpha(T)] = \text{const}$. Note that the value of the constant is irrelevant as the shape of the relaxation barely evolves with temperature for a given value of K, as long as the constant corresponds to the final decay. We use the value 0.28 which lies roughly in the middle of the final relaxation for large K. The temperature dependence of the corresponding $\tau_\alpha(T)$ is presented in Fig. 2 using an Arrhenius plot [see Fig. 2(a)] and using a reduced plot inspired by the mode-coupling prediction [see Fig. 2(b)]. These results confirm that for the largest range studied, $K = 24$, the dynamics is very close to the results obtained directly on the Bethe lattice [58], which were shown to obey a power-law divergence,

$$\tau_\alpha(T) \propto |T - T_c|^{-\gamma}, \tag{6}$$

with $\gamma = 2.9$ and $T_c \simeq 0.481$. This temperature is indicated with a vertical line in Fig. 2. When plotted as a function of $T - T_c$ in a log-log representation, the data for $K = 24$ follows the power-law divergence over almost the entire temperature regime we were able to study numerically. We observe a power-law regime over nearly four decades of slowing down, which is more than what is typically observed in supercooled liquids.

When K is decreased, however, stronger deviations from this power-law divergence appear, and the deviations appear at higher temperatures when K becomes smaller. Accordingly, the mode-coupling power law is obeyed over a range which shrinks with decreasing K [see Fig. 2(b)]. For $K = 1$, the power law is followed over about two decades only, which means that the system is quite far from its mean-field limit. In fact, without the $K = 24$ data as a guide, it would be difficult to argue that a mode-coupling crossover occurs at all for this system [50], a situation which we will again encounter in Sec. V when considering off-lattice systems. Note that, in this analysis, we have not tried to use T_c as an additional free parameter, which would somewhat improve the quality of the power-law fit.

These results clearly show that relaxation in the KFA model is a combination of mode-coupling and cooperative dynamics, whose respective importance depends on the temperature, the geometry of the underlying lattice (i.e., the value of K), and the considered time scale. For large values of K we find an apparent mode-coupling divergence analogous to the one reported for the Bethe lattice with the same connectivity. However, in contrast to Bethe lattices, the dynamic singularity is eventually avoided for *any* value of $K < \infty$. This can be proven rigorously, the argument being deferred to the Appendix. The proof for $K > 1$ is a straightforward generalization of the $K = 1$ case discussed previously [59], and it shows that for any finite K the relaxation time diverges only at $T = 0$, with a divergence which becomes steeper when K increases. This results from the behavior of the upper bound we derive for $\tau_\alpha(T)$, showing that $\tau_\alpha(T)$ cannot grow faster than $\exp[K \exp(K/T)]$, to leading order at low T.

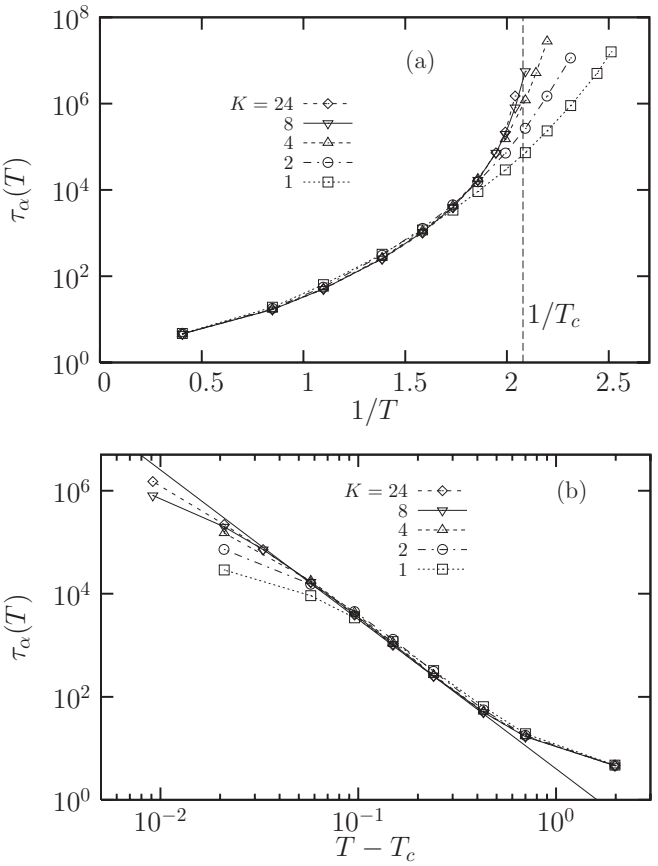

FIG. 2. Temperature evolution of the relaxation time in the KFA model. (a) Arrhenius plot; the vertical line is at $T_c(K = \infty) = 0.480898$. (b) The same data plotted in a log-log representation as a function of $T - T_c$; the full line represents the mean-field limit given by Eq. (6). In both panels, we see that deviations from mean field occur at higher T for smaller K, which shrinks the domain of validity of the mean-field prediction for the growth of τ_α.

Interestingly, this argument also suggests that by using any of the standard definitions of the kinetic fragility, the KFA model would become more fragile with increasing value of K, with the fragility even becoming formally infinite when $K \to \infty$. The fragility increases with K because the dynamics is more influenced by the mode-coupling crossover and closer to an algebraic singularity at T_c, which is responsible for the fragility increase observed numerically in Fig. 2. In the low-temperature regime below the mode-coupling crossover where the upper bound derived in the Appendix is valid, the corresponding fragility also increases because the effective activation energy increases with K. Within the KFA

model, we arrive at the intriguing conclusion that systems where the mode-coupling crossover is more pronounced are also characterized by a larger kinetic fragility. It would be interesting to know whether such a correlation holds for real supercooled liquids. We discuss this issue further in Sec. V.

C. Dynamical finite-size effects

Having established that the KFA model smoothly interpolates between mode-coupling and cooperative dynamics, we are now in a position to study how the different regimes are affected by confinement and the corresponding finite-size effects. In order to do that, we shall analyze how the alpha relaxation depends on the control parameters (K,T,L). We recall that, for small system sizes, instances containing a blocked backbone may appear with a finite probability. When this probability becomes large, the KFA model is no longer a physical description of realistic glassy liquids, which cannot be truly blocked. In a more realistic system, a different relaxation mechanism will replace facilitation. In order to avoid this problem, we have decided to reject those instances and perform an average over samples which do not contain blocked backbones.

We find that the shape of the persistence functions depends weakly but in a nontrivial manner on the control parameters. For this section we use, for convenience, an integral definition of the relaxation time:

$$\tau_\alpha = \int_0^\infty dt\, P(t). \tag{7}$$

We have checked that our conclusions do not depend on this particular definition of τ_α. We have explored the dependence of τ_α on all three parameters over a wide range. We now present the salient features of the finite-size effects within the KFA model.

First, we fix the temperature and study how the relaxation time reaches its bulk value for $L \to \infty$ for different connectivity ranges K (see Fig. 3). For a moderate temperature, $T = 0.577$ (recall that $T_c = 0.481$), bulk relaxation times are of the order 5×10^3 for all K. We observe that this value is reached for moderate system sizes in all cases, $L \approx 20$–40, and that the $K \to \infty$ limit is reached very quickly as well, since the data do not change for $K \geqslant 8$. Strikingly, we find that the asymptotic value of $\tau_\alpha(L)$ is reached from below for $K = 1$ and from above for $K \geqslant 4$, suggesting that finite-size effects are qualitatively different for mode-coupling ($K > 4$) and cooperative ($K < 4$) regimes at this temperature.

These observations are amplified at lower temperature. For $T = 0.502$, bulk dynamics is recovered only at much larger system sizes, from $L \approx 30$ for $K = 1$ to $L \approx 150$ for $K = 24$. Moreover, since we are very close to the mean-field singularity, the $K \to \infty$ limit is only achieved for much larger K, near $K \approx 32$. Thus, by decreasing the temperature we observe enhanced finite-size effects in both dynamical regimes, which constitutes direct evidence that dynamical slowing down is accompanied by a growing correlation length scale and unveils the existence of a growing length $\ell_{\rm FS}(T)$, which determines dynamical finite-size effects and which grows by lowering the temperature. We emphasize that this result holds both in mean-field and cooperative regimes even though the system size dependence is qualitatively different in the two cases.

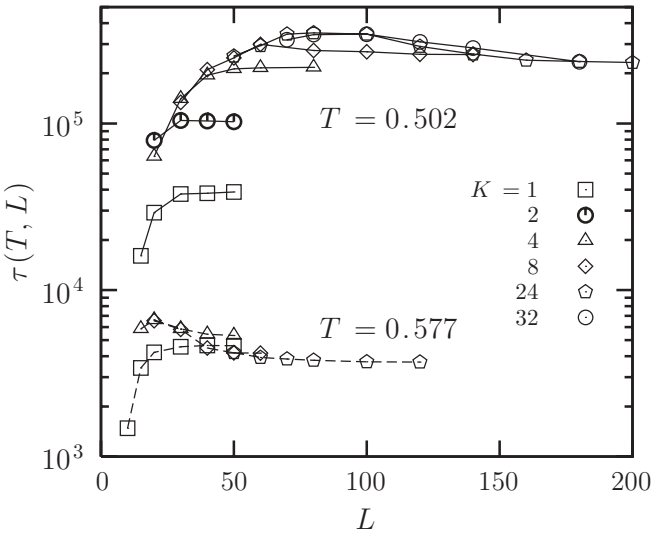

FIG. 3. System size dependence of the relaxation time in the KFA model at two fixed temperatures and various values of the interaction range K. The strong temperature evolution of the finite-size effects indicates the growth of $\ell_{\rm FS}(T)$ at low T. Note the different L dependence in the cooperative (τ_α increases with L) and the mode-coupling (τ_α decreases with L) regimes.

We now fix the connectivity range K and study for each different K value the whole temperature evolution of the finite-size effects in Fig. 4. For the case $K = 1$, shown in Fig. 4(a), the mode-coupling regime is almost absent and the dynamics appears to be activated and of non-mean-field type in the whole slow dynamics regime. Correspondingly, the relaxation time increases with L for all temperatures with no sign of nonmonotonic behavior. This behavior can be explained by recalling that relaxation in the $K = 1$ model proceeds via diffusion of so-called macro-vacancies. The relaxation time corresponds to the time it takes a macro-vacancy to diffuse over an area comparable to the inverse of the macro-vacancy density. When the system size becomes smaller than this characteristic area dynamical finite-size effects set in. The interpretation is that by sampling configurations that do not contain blocked structures, we are effectively conditioning the sampled configurations to always contain at least one macro-vacancy. The area over which this macro-vacancy must diffuse becomes smaller when L decreases, and so does the relaxation time. This argument also explains why convergence to the bulk behavior is reached only at system sizes that grow with decreasing T, because the density of macro-vacancies decreases. Therefore, the growth of $\ell_{\rm FS}(T)$ is directly related to the growth of dynamical correlations in this regime which directly control the finite-size effects observed in Fig. 4(a).

The situation for $K = 4$, shown in Fig. 4(b), is different because mode-coupling dynamics now controls the relaxation over an intermediate temperature regime, as discussed above. We have argued in Sec. III C that mode-coupling dynamics in finite systems should be slower than in the bulk, which is indeed compatible with the higher temperature data shown in Fig. 4(b), which show that the bulk value of the relaxation time is reached from above. This situation is in stark contrast

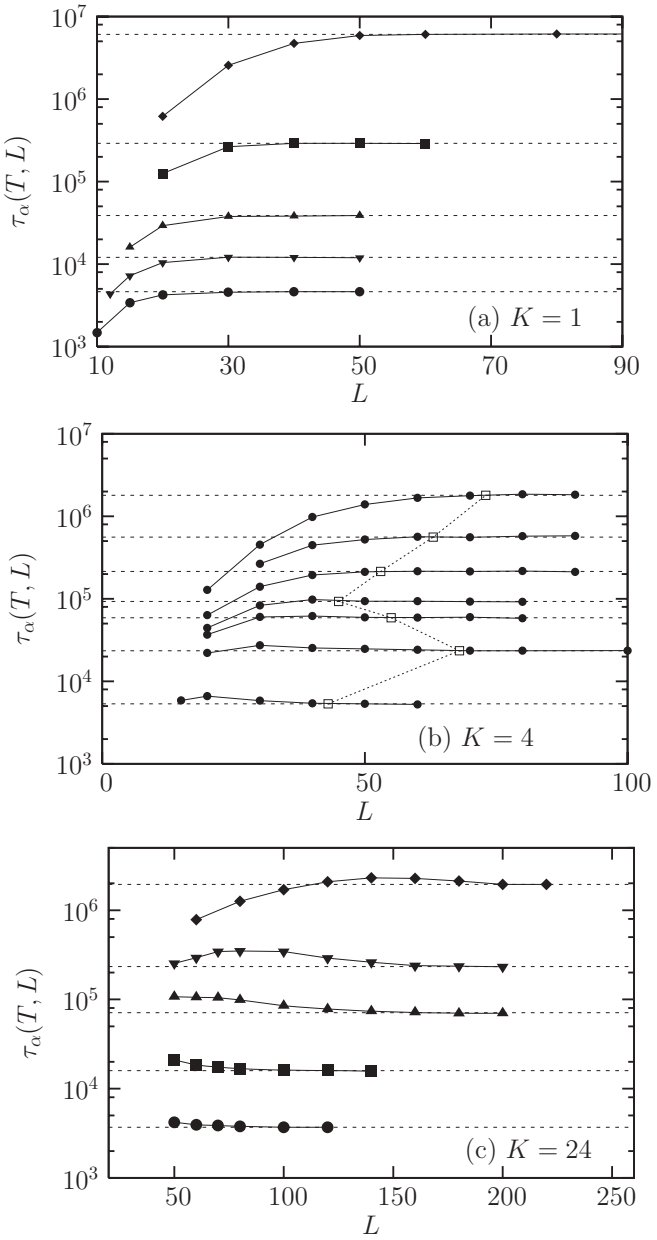

FIG. 4. Temperature evolution of finite-size effects. (a) $K = 1$ and various temperatures: $0.577 \leqslant T \leqslant 0.409$. (b) $K = 4$ and various temperatures: $0.577 \leqslant T \leqslant 0.490$. (c) $K = 24$ and various temperatures: $0.577 \leqslant T \leqslant 0.490$. While τ_α grows with L in the purely cooperative regime ($K = 1$ at all T, $K = 4$ at low T), it decreases with L in the mode-coupling regime ($K = 4$ and 24 at moderate T) and has a nonmonotonic size dependence when both regimes coexist and compete ($K = 4$,24 near T_c). This competition produces a nonmonotonic temperature evolution of the characteristic length $\ell_{\rm FS}(T)$, indicated by open symbols in (b).

with the cooperative behavior obtained for $K = 1$ in Fig. 4(a). Decreasing the temperature has two effects. First, bulk dynamics is reached only at system sizes that grow, because $\ell_{\rm FS}(T)$ grows, as noticed above. Second, the presence of the mode-coupling regime becomes evident, as dynamics becomes cooperative and thus reacts differently to finite sizes. At very low temperature we find that dynamics is fully cooperative, and τ_α increases with L. A striking behavior is observed near $T \approx T_c$ where both types of dynamics coexist and compete to yield a nonmonotonic behavior of $\tau_\alpha(L)$, which should be interpreted as a mixture of high- and low-temperature behaviors.

A second striking consequence of this competition is that the length $\ell_{\rm FS}(T)$, which can be estimated as the system size needed for $\tau_\alpha(L,T)$ to converge to the bulk value, has a nonmonotonic evolution with temperature, as indicated by the open symbols in Fig. 4(b). These open symbols have been placed in between the first two consecutive L values for which the relaxation time no longer evolves, within statistical accuracy. While these points do not represent the result of the quantitative determination of a characteristic system size, they describe qualitatively well the numerical data. This behavior occurs near the mode-coupling temperature and the minimum of $\ell_{\rm FS}(T)$ occurs when the opposite effects of cooperative and mode-coupling dynamics on the relaxation time nearly compensate to produce negligible finite-size effects. The effective nonmonotonic temperature evolution of $\ell_{\rm FS}(T)$ is strongly reminiscent of the numerical findings of Ref. [31], as we discuss further in Sec. VI. By contrast, the four-point dynamic susceptibility measured in the bulk does not show such a nonmonotonic temperature evolution, as discussed in the Appendix.

We were only able to detect such a nonmonotonic temperature evolution of $\ell_{\rm FS}(T)$ over a narrow range, $4 \leqslant K \leqslant 8$. This is because small K values are little influenced by the mean-field limit, while for large K we cannot study low enough temperatures and enter the fully cooperative regime. Indeed, for $K = 24$, shown in Fig. 4(c), we find a qualitatively similar coexistence and nonmonotonic behavior at intermediate temperatures, and the effect is even more pronounced because, for this K value, the mode-coupling singularity is only narrowly avoided, and the mode-coupling regime extends to much lower temperatures. However, for this value we have not been able to reach sufficiently low temperatures to see purely cooperative dynamics and a monotonic increase of τ_α with L [see the lower temperatures in Fig. 4(c)].

In conclusion, the study of finite-size effects in the KFA model, where the relative importance of mode-coupling and cooperative dynamics can be controlled, supports the validity of the theoretical arguments developed in Sec. III. We find in particular that both temperature regimes exhibit qualitatively distinct responses to the use of finite sizes, while in the crossover region a remarkable nonmonotonic size dependence is obtained, which reveals in a very direct manner that the nature of the relaxation is changing near the avoided singularity T_c. We also observe that for systems that are too far from the mean-field limit, this crossover is too weak, dynamics is mostly controlled by cooperative processes, and τ_α increases monotonically with L. Therefore, finite-size effects can be viewed as a powerful tool to probe the existence of a physically relevant temperature regime where mean-field-like dynamics prevails. In all cases, we find that finite-size effects appear for $L \leqslant \ell_{\rm FS}(T)$, where $\ell_{\rm FS}(T)$ represents a length scale which grows upon decreasing the temperature in both mode-coupling and cooperative regimes, but exhibits an apparent nonmonotonic temperature evolution when the opposite effects of mean-field and cooperative dynamics nearly compensate.

V. RESULTS FROM MOLECULAR DYNAMICS SIMULATIONS

A. Models and bulk behavior

Given the diversity of behaviors predicted theoretically in previous sections, we have decided to undertake a large numerical effort to investigate finite-size effects in a broad variety of model systems using molecular dynamics simulations and to study liquids with different interactions and kinetic fragilities. We have performed large-scale simulations of four model liquids representative of different classes of systems.

The first model, which we call the "network liquid," was introduced and studied in Ref. [66]. By using carefully chosen Lennard-Jones interactions between the two components of a binary mixture, it is possible to mimic the structure of network-forming liquids (such as silica) while avoiding the use of long-range electrostatic interactions, which is especially convenient when small systems need to be studied. Additionally, at low enough temperatures the temperature dependence of the relaxation time was found to be close to an Arrhenius law [66], and therefore we use this network liquid as representative of the class of strong glass-formers.

The second model we study is the binary Lennard-Jones mixture introduced in Refs. [67]. The model was originally devised as a simple Lennard-Jones model for two-component metallic glasses and has become a canonical system for numerical studies of supercooled liquids [68]. Its relaxation time grows in a super-Arrhenius manner, and so it is considered as a good model for fragile liquids. Although comparing kinetic fragilities between simulations and experiments is not straightforward, the binary Lennard-Jones mixture has an "intermediate" fragility, which suggests it is less fragile than typical fragile glass-forming materials studied in experiments such as for instance ortho-terphenyl [66,69].

The third model is also a canonical model for studies of the glass transition. It is a binary mixture of soft spheres interacting with a purely repulsive r^{-12} potential introduced in Ref. [70]. Its behavior is in fact very similar to the one of the binary Lennard-Jones potential, since this model also seems to display an intermediate kinetic fragility.

The fourth model we study is a binary mixture of soft repulsive particles interacting with a one-sided repulsive harmonic potential. The model was introduced in Ref. [71] as a model for wet foams, and its glass-forming properties were studied in Refs. [72], where it was shown that, over a broad regime of densities, this system actually behaves as a quasi-hard-sphere system. Comparing the kinetic fragility of hard spheres (whose glass transition is controlled by density) to molecular liquids (controlled by temperature) is ambiguous [72]. However, using the compressibility factor $Z = P/(\rho T)$ to build the analog of an Arrhenius plot for hard spheres [72] suggests that hard spheres are actually characterized by a rather large kinetic fragility. We take harmonic spheres as being representative of fragile glass-forming materials.

Because these models have been studied extensively before, we only provide limited details about our simulations in the sections below, and we refer to the original publications for more information. Our focus in this work was to analyze how simulations in finite-size systems differ from the bulk behavior, and whether the observed finite-size effects could be interpreted along the lines discussed in previous sections. As a dynamical observable the behavior of the self-intermediate scattering function, $F_s(q,t)$, is measured, and we determine the alpha-relaxation time $\tau_\alpha(T)$ from the time decay of this correlator to the value $1/e$ and a wave vector corresponding to the first peak of static structure, as is usual [1]. Our central aim is to measure $\tau_\alpha(T,N)$ for systems containing a finite number of particles, N.

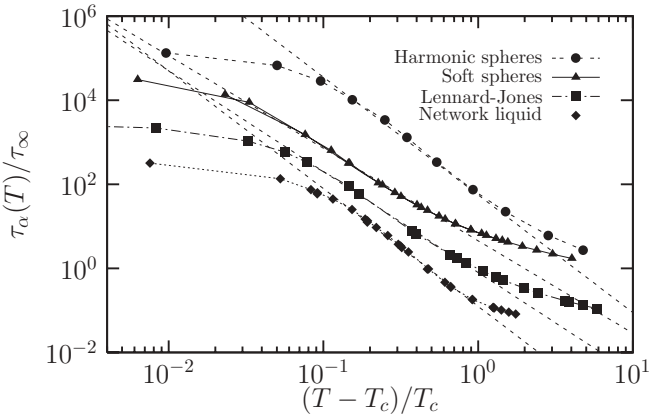

FIG. 5. Bulk relaxation time $\tau_\alpha(T)$ of the four model liquids studied in this work using the representation of Fig. 2(b) appropriate for detecting a mode-coupling algebraic divergence at temperature T_c. We vertically shift the systems by a time constant τ_∞ for clarity, and show as a dashed line the result of power-law fits with exponents $\gamma = 2.8$, 2.4, 2.2, and 2.8 for the network liquid, Lennard-Jones particles, and soft and harmonic spheres, respectively. The power-law fit is obeyed over a broader range from bottom to top.

By construction, simulations are performed in a temperature regime which corresponds to the first four to five decades of dynamical slowing down. Thus, this regime is typically the one where predictions from the mode-coupling theory are usually tested. Therefore, our simulations fall in the temperature range where a crossover from mode-coupling to activated dynamics might occur. In Fig. 5 we give evidence that such a crossover seems to be present in the bulk dynamics of the four liquids. For all liquids, we measure the temperature dependence of the bulk relaxation time. We then fit its temperature evolution to a power-law divergence, as in Eq. (6), to estimate the location T_c of the mode-coupling singularity. We present the data for the four liquids in Fig. 5 using the same representation as in Fig. 2(b), where a power-law divergence appears as a straight line. For all liquids, a power-law regime is obtained for intermediate temperatures, although the time window over which it applies depends on the particular system. Unsurprisingly, we find that a power-law divergence is not very pronounced for the network liquid which rapidly enters an Arrhenius regime at low temperatures, while the harmonic sphere system is the one for which the power law is the most convincing. The Lennard-Jones and soft-sphere mixtures have an intermediate behavior. Thus, we find that the degree to which mode-coupling theory predictions apply (at least for the bulk relaxation time) seems correlated with the kinetic fragility of the model. The same connection was found in the KFA model in Sec. IV. We emphasize that a power-law fit to the relaxation for moderately supercooled liquids is bound to

yield a quantitative estimate of the value of T_c, but this does not necessarily imply, as we shall see, that the long-time dynamics is truly controlled by the mode-coupling physics [50].

B. Network liquid with Arrhenius behavior

We start our discussion with the results obtained for the network liquid [66]. The model is an AB_2 binary mixture designed to be a simple analog of silica, SiO_2, forming a connected assembly of tetrahedric structures. For this system, we find that dynamics becomes slow when temperature becomes smaller than $T \approx 0.45$, and we can follow finite-size effects down to $T = 0.29$, where bulk dynamics has slowed down by about four decades. Using a power-law fit of these data, we obtain an exponent $\gamma \approx 2.8$ and extract the location of the mode-coupling temperature, $T_c \approx 0.31$. Since the power law is obeyed over a limited temperature range, it is relatively easy to access temperatures lower than T_c in equilibrium conditions, as found also in a more realistic model of silica [73]. The density of the system, $\rho = 1.655$, has been adjusted to best reproduce the structure of silica obtained in molecular dynamics simulations performed at density $\rho = 2.37$ g/Å^3 [73].

For this system we performed simulations both using a thermostat (in the NVT canonical ensemble [74]) and without a thermostat after proper thermalization (in the NVE microcanonical ensemble), because as discussed in Refs. [75] thermally activated processes for systems evolving with Newtonian (i.e., energy-conserving) dynamics might induce dynamical correlations between particles when the heat needed to cross a barrier locally is borrowed from neighboring particles. We found no quantitative differences between the two sets of simulations, and we have therefore merged the two sets of simulations for the bulk data presented in Fig. 5.

The results corresponding to dynamical finite-size effects are reported in Fig. 6, where both NVT and NVE simulations are shown, yielding quite similar results. We use system sizes

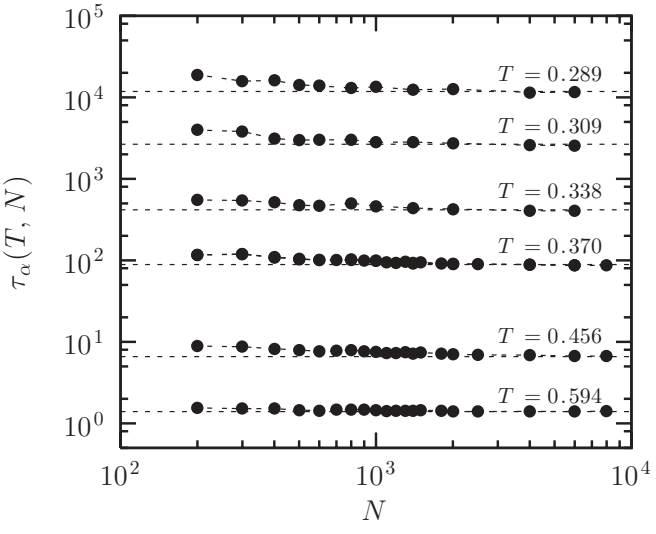

FIG. 6. System size dependence of relaxation time in the network liquid where $T_c \approx 0.31$. The dynamics slows down for smaller systems, but the amplitude and range of the effect evolve weakly with temperature.

that are limited on the small-N side by the fact that the static structure, as revealed by the pair correlation function $g(r)$, becomes sensitive to N and the network of tetrahedra does not fit well the small simulation box. For large N, we easily observe convergence to the bulk behavior for the relaxation time as soon as N is larger than a few thousand particles. In Fig. 6 we observe a small finite-size effect, since $\tau_\alpha(T,N)$ reaches its bulk value from above; that is, small systems are slower than larger ones. However, this effect is quite modest and, more importantly, it does not seem to evolve very much over the temperature range where slow, Arrhenius dynamics is observed, i.e., $T \leqslant 0.45$. Therefore, for the network liquid, we find no clear evidence that the length scale $\ell_{\rm FS}(T)$ becomes large at low temperatures. These results are consistent with the view that, for systems showing an Arrhenius behavior, relaxation remains "local" and that correlations are rather weak and evolve very slowly with the temperature [76].

Dynamic heterogeneity has not been studied in detail for the present network liquid, but growing four-point dynamic susceptibilities (but not dynamic length scales) have been reported in numerical studies of silica [77,78]. A way to reconcile these findings with our result is either that $\ell_{\rm FS}(T)$ is not related to the dynamical correlation length or that dynamic susceptibilities grow at low temperatures because the strength, rather than the spatial extent, of dynamic correlations increase at low T, a point that deserves further study.

Contrary to what was found for the activated (and highly cooperative) regime of the KFA model, the small dynamical finite-size effect reported for the network liquid goes in the opposite direction of making the dynamics slower for smaller systems, which indicates that this finite-size effect is not related to a competition between the system size and the spatial extent of the relaxing "entities." A possible explanation is that, for small system sizes, the silica-like network is somewhat frustrated by the periodic boundary conditions, which could increase slightly the energy barrier needed to form a defected tetrahedra, and thus slow down the dynamics. In this view, dynamical finite-size effects would be dominated by noncollective effects and, possibly, related to a subtle change of the static structure, an issue worth pursuing.

C. Binary Lennard-Jones mixture

We now turn to the case of the binary Lennard-Jones mixture [67]. This model displays super-Arrhenius relaxation, and it is a model for which several quantitative tests of the scaling predictions of the mode-coupling theories have been performed with some success [67], even though deviations from the predictions can be observed at low temperatures [75]. Additionally, growing dynamic length scales have been reported for this system [79–83]. For all these reasons, one may expect a more interesting temperature dependence of finite-size effects for this model.

The results of our molecular dynamics simulations are shown in Fig. 7. The simulations were performed in the microcanonical ensemble only, the value of the total energy being carefully controlled in each independent simulation to maintain the temperature equal to the desired value and

prevent spurious fluctuations in the dynamics. We present data for the high-temperature liquid, $T = 2.0$, and below the onset of glassy dynamics, $T \approx 1.0$, down to $T = 0.42$, which lies below the fitted value of the mode-coupling temperature $T_c \approx 0.435$ [67].

We find that almost no dynamical finite-size effects are present above and near the onset temperature for slow dynamics, consistent with the idea that, in simple liquids, relaxation is a fast local process. For $0.5 \leqslant T \leqslant 1.0$, we find that finite-size effects are present at small sizes and that the dynamics slows down when N is small [9]. Remarkably, we find that this effect becomes more pronounced both in amplitude and in range, suggesting that the interplay between system size and structural relaxation has a more collective nature than in the Arrhenius liquid studied in Sec. V B. This suggests that a nontrivial characteristic length scale $\ell_{\rm FS}(T)$ grows when temperature is decreased below the onset temperature of this model, in agreement with previous work [15,16]. Repeating the empirical analysis performed recently in Ref. [16], we find similarly that the typical length scale over which finite-size effects occur grows by about 50% over the temperature range $T = 0.42$–1.0. In contrast to previous work [15], however, we always find a monotonic N dependence of τ_α, even at low temperatures. We believe that the (relatively small) nonmonotonic size dependence reported earlier [15] was due to statistical uncertainty [84].

Another result obtained below T_c is that we do not find a qualitative change in the size dependence of the relaxation time and the bulk value is still reached from above by increasing L for this low temperature. Therefore, contrary to what has been found for the KFA model or predicted on general grounds for activated relaxation, we do not find any nonmonotonic behavior near or below T_c. We find this result somewhat surprising and suggest several hypotheses to account for these observations. First, it could be that the mode-coupling crossover is absent or very weak in this case, as in the network liquid studied above. This is however at odds with previous work establishing the validity of the scaling predictions of mode-coupling theory for this system at intermediate temperatures [67]. The second hypothesis is that activated dynamics at low temperatures involves a cooperativity length that has not yet grown very large, and thus it cannot compete with the system size L before other, more microscopic effects, also appear such that there is no room for the general argument of Sec. II to apply. By this argument we would conclude that much lower temperatures should be studied to reveal a change in the nature of finite-size effects in this model, which is at present beyond our numerical capabilities. A possible interpretation is that static point-to-set correlation length scales do not grow significantly in this system over the temperature regime currently accessible to simulations, or at least much less than dynamical correlation length scales. See Refs. [27,85,86] for recent work on static correlations in this system.

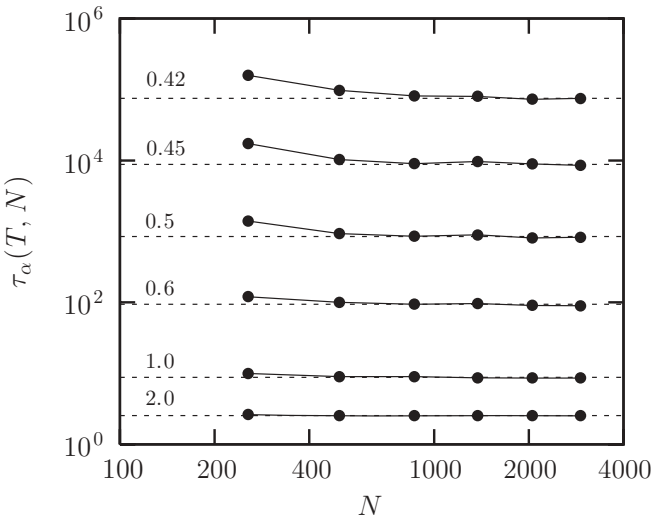

FIG. 7. System size dependence of relaxation time in a Lennard-Jones liquid from the high-temperature liquid, $T \geqslant 1.0$, down to below the mode-coupling temperature $T = 0.42 < T_c \approx 0.435$.

D. Soft spheres

In this section we study the binary system of soft spheres introduced long ago in studies of the glass transition [70]. We choose the particular model studied by several groups [25,70,87,88], namely, a 50:50 mixture of soft spheres interacting with an r^{-12} repulsion, with different species having different sizes. We use a diameter ratio of 1.2 and adopt the same units as in Ref. [25], where density ρ is fixed and temperature T decreased (although this is a matter of convenience for this system since the static structure is uniquely controlled by the combination $\Gamma = \rho T^{-1/4}$). It was shown that this model displays in the supercooled regime increasing dynamic [88] and static [26] length scales. We perform simulations in the canonical NVT ensemble, using a Nosé-Poincaré thermostat with inertia parameter $Q = 5.0$ [74].

A new technical difficulty for this system is that its glass-forming ability is worse than the three other models studied in this work. In particular, we found that crystallization intervenes very easily when temperature is decreased, especially in small systems. Thus, we had to carefully determine for each independent sample whether or not it had crystallized in the course of the simulation. We did so by measuring several structural indicators, such as pressure, energy, and pair correlation function, from which crystallization was obvious. Therefore, in the data presented below, we only consider state points where crystallization was found very infrequently. In practice, we do not show data when crystallization occurred in more than 30% of the samples.

A few of the remaining data are still a little ambiguous, as we observe fluctuations of the potential energy that are large and long-lived but do not correspond to an irreversible crystallization of the system. This is reminiscent of the numerical observations reported for another binary mixture [89]. For these runs, dynamics is typically slower than the average, and it is not clear whether these runs should be discarded (as being affected by incomplete crystallization) or averaged together with "normal" samples (as being characterized by some other forms of local ordering). We checked that the main conclusions reported below are not affected if we remove these very slow samples.

For this system, the bulk data were fitted to a power-law divergence, and the result of this fitting is shown in Fig. 5,

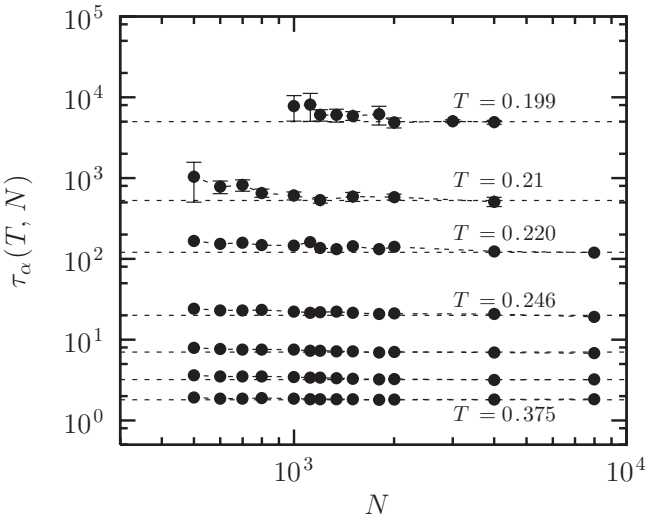

FIG. 8. System size dependence of relaxation time in a soft sphere mixture from the high-temperature liquid, $T \geqslant 0.25$, down to the mode-coupling temperature ($T_c \approx 0.198$). We only consider state points where crystallization is very infrequent. The overall temperature evolution is similar to the Lennard-Jones results in Fig. 7.

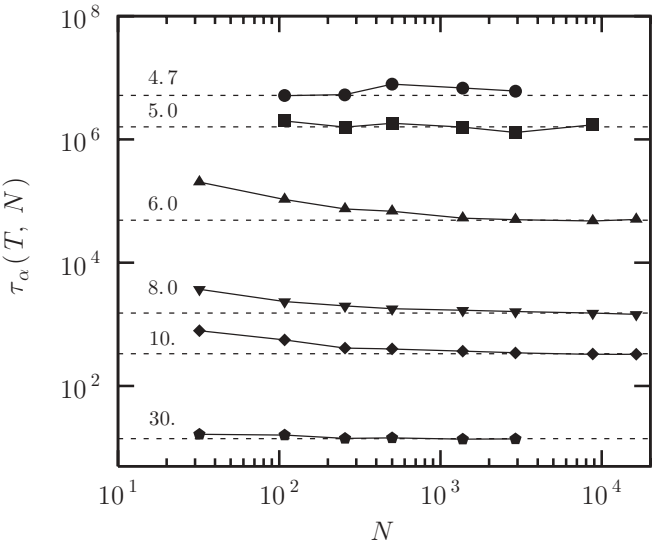

FIG. 9. System size dependence of relaxation time in a harmonic sphere mixture from the high-temperature liquid, $T \geqslant 13$, down to the mode-coupling temperature $T_c \approx 5.2$. Note the qualitative change of size dependence near the mode-coupling crossover and the nonmonotonic size dependence at low T.

where we use $\gamma \approx 2.2$ and $T_c \approx 0.198$. We note that this value is significantly smaller than the values ($T_c = 0.226 - 0.246$) quoted in the literature [25,28,87,90], which stem from very early work [87] and presumably overestimated the mode-coupling temperature by a very large amount.

We present our results for finite-size effects in the soft-sphere mixture in Fig. 8. As for the Lennard-Jones model, we find that dynamics is rather insensitive to system sizes in the high-temperature liquid but becomes size dependent below the onset of glassy dynamics, which we locate near $T \approx 0.25$. The size dependence also extends to larger sizes when T decreases, signalling again the growth of the characteristic length $\ell_{\rm FS}(T)$ with decreasing T. Unfortunately, due to the crystallization issue mentioned above, it is not easy to follow the size dependence to very low temperatures over a broad range of system sizes. The limited amount of data shown in Fig. 8 seems to suggest that soft spheres have a behavior similar to the one observed in the Lennard-Jones system. In particular, the size dependence for $T = 0.2$, near the mode-coupling temperature, does not show sign of a qualitatively different behavior as compared to higher temperatures. We were not able to study this system at even lower temperatures, because of crystallization issues. We suspect in particular that the very strong finite-size effects reported in Ref. [10] might be affected by crystallization as well, since the size dependence reported in Fig. 8 is more modest.

E. Harmonic spheres

The final model we consider is a 50:50 binary mixture of harmonic spheres with diameter ratio of 1.4, which we study using molecular dynamics simulations in the microcanonical ensemble. We use the same parameters as in Ref. [31] and work at constant density $\rho = 0.675$ and use temperature as a control parameter. For this density, the onset of glassy dynamics is near $T \approx 13$ and the mode-coupling temperature used in Fig. 5 is $T_c \approx 5.2$ [31,72]. In contrast with the soft-sphere model studied in the previous section we find that crystallization is not an issue for systems as small as $N = 108$ over the entire range of temperatures. Since the range of the potential is equal to the particle diameter (as for hard spheres), we can in principle study even smaller system sizes. We have found that this is only possible for large enough temperatures, with systems with $N = 32$ becoming very heterogeneous at low temperatures. Therefore, we shall only display data for those state points where stability is never an issue.

In Fig. 9 we present our results for the finite-size dependence of the relaxation time in harmonic spheres across the mode-coupling crossover. For high and moderately low temperatures, we find results that are qualitatively very similar to the ones discussed in the previous sections for soft and Lennard-Jones particles, with no size dependence above the onset and a slowing down at small sizes between the onset and mode-coupling temperatures which becomes more pronounced if T is lowered.

Strikingly, we find that near and below the mode-coupling temperature the size dependence changes its qualitative form to become nearly size independent at $T = 5.0$, and even nonmonotonic with N at the lowest temperature we have been able to study, $T = 4.7$. For this temperature, we note that the maximum of $\tau_\alpha(N)$ occurs for a system size of about $N \approx 600$, where the structure is very stable and very close to that found in the bulk system. Additionally, these data have been averaged over a large number of realizations and very long simulation times to reduce the statistical noise, and so the effect reported in Fig. 9 is physical.

The data presented in Fig. 9 are qualitatively similar to the one obtained for the KFA model at intermediate K [see Fig. 4(b)] and presumably have a similar physical origin. A natural interpretation of this nonmonotonic behavior comes from the fact that it occurs very close to the fitted

mode-coupling temperature, $T_c \approx 5.2$, where deviations from mode-coupling predictions are already present (see Fig. 5). Therefore, we attribute this change of behavior to a change of physical mechanism controlling the relaxation from mode-coupling to activated dynamics.

From the behavior shown in Fig. 9 we conclude also that mode-coupling and activated dynamics interact and compete to produce an apparently nonmonotonic temperature evolution of $\ell_{\rm FS}(T)$, having a maximum near $T \approx 6$ and a minimum near $T \approx 5$ (see Fig. 9). It is remarkable that this qualitative evolution with temperature of $\ell_{\rm FS}(T)$ follows very closely the behavior reported for dynamic profiles near an amorphous wall in Ref. [31] for the same system. Thus, we think that the bulk data reported in Fig. 9 provide both an independent confirmation and a natural physical interpretation of the surprising nonmonotonic dependence of dynamic length scales found near T_c in this system [31].

Finally, for the system of harmonic spheres, we have additionally studied the dynamics using Monte Carlo simulations, using the same implementation as in Ref. [91]. For the present system we found that Monte Carlo dynamics is slightly less efficient than molecular dynamics, so that getting data comparable to those shown in Fig. 9 is challenging. Instead, we performed very long simulations for only a few selected state points (N,T), which confirmed that, also for Monte Carlo dynamics, the size dependence of the relaxation time becomes nonmonotonic at low temperature, $T = 4.7$, and nearly size independent at $T = 5$, in agreement with Fig. 9. Therefore, this effect is not due to the specific type of dynamics chosen to perform our study. This also confirms that hydrodynamic effects [41,42] play very little role in the results presented in this work.

VI. SUMMARY AND CONCLUSION

To conclude this article, we wish to summarize the main results obtained in this work. First, we discussed from a theoretical point of view the possible effects and the interest in using small sizes to study the dynamics of supercooled liquids. We presented the following arguments, which depend on the precise mechanism envisioned for structural relaxation in systems approaching the glass transition.

(1) Only minor finite-size effects are expected for strong glass-formers whose relaxation time follows an Arrhenius law because the corresponding activation energy likely corresponds to a "local" excitation. Thus, the length $\ell_{\rm FS}$ should not grow with decreasing temperature and the relaxation time scale for small system sizes should be dominated by nonuniversal effects affecting the local energy barrier for relaxation.

(2) For cooperative, thermally activated processes, dynamics becomes faster if the system size decreases because cooperative events then involve a smaller number of particles, thus reducing the barrier for relaxation. In this case the growth of $\ell_{\rm FS}$ should track the one of the length scale measuring cooperativity (e.g., the point-to-set length within RFOT theory).

(3) Mode-coupling relaxation becomes slower in smaller systems because spatially extended, unstable relaxation modes become stable in small systems [40]. This trend holds until activated dynamics takes over when all unstable modes have disappeared, and presumably makes relaxation faster as described in item 2. Overall, the size dependence can thus be nonmonotonic at intermediate temperatures. Moreover, this can lead to a quite unusual behavior of $\ell_{\rm FS}(T)$ that would track that of the dynamical correlation length.

(4) For diffusing point defects, dynamics becomes slower when system size decreases because another relaxation channel must be used when no defects are present in small systems. If cooperative activation occurs, then the dynamics may accelerate at small sizes, making the overall size dependence nonmonotonic. In this case $\ell_{\rm FS}(T)$ is expected to be related in a power-law way to the dynamical correlation length.

(5) For kinetically constrained models, defects are the only channel available. Thus, dynamics becomes nonergodic in samples containing no defects, which can be seen as an extreme slowing down. By discarding these instances, one biases the statistical weight toward configurations with larger concentration of defects, and as a result the measured relaxation time decreases when the system size decreases (the effective defect concentration increases).

We have also introduced a lattice glass model, the Kac-Fredrickson-Andersen model, for which the distance to the mean-field (or mode-coupling-like) limit can be controlled by tuning the range K of the spin connectivity. We have provided numerical and analytical evidence that this approach successfully generates an avoided mode-coupling singularity, in analogy with real supercooled liquids. The detailed analysis of the dynamical finite-size effects of this model agrees with the general theoretical predictions. For $K = 1$, we obtain a monotonic growth of the relaxation time with system size, explained by mechanism 5. However, for intermediate values of K, the system exhibits an MCT crossover and the behavior follows a nonmonotonic size dependence. Although here the reason for nonmonotonicity is not that small systems have activated dynamics, the study of the KFA model is a concrete example for which one finds that the interplay between two competing relaxation mechanisms can lead, for intermediate K values, to a surprising nonmonotonic temperature evolution of the characteristic length $\ell_{\rm FS}(T)$.

Subsequently, we have presented the results of simulations of four models for supercooled liquids. Mechanism 1 gives a good description of the size dependence for the strong, network-forming liquid. The effect of the mode-coupling crossover described by mechanism 3 is observed in a model of quasihard spheres, while the behavior of the Lennard-Jones and soft-spheres models appeared somewhat intermediate between mechanisms 1 and 3 and was harder to interpret.

Overall, the simulation of fragile systems seem to confirm the RFOT result of Ref. [40], recently discovered in simulation of model systems [31], that dynamic and static length scales are largely decoupled in the mode-coupling regime and have distinct temperature dependencies, with static point-to-set length scales starting to show a significant growth at temperatures near the mode-coupling crossover, while dynamic length scales grow rapidly even at higher temperatures. A natural interpretation of the nonmonotonic size dependence found in Fig. 9 is that both types of mechanisms compete near the mode-coupling temperature. This competition has also been invoked to interpret the nonmonotonic behavior of dynamic

profiles near an amorphous wall in Ref. [31]. We have shown that a similar nonmonotonic temperature evolution of $\ell_{\rm FS}(T)$ is obtained in the same harmonic-sphere model.

These results contribute to a clarification of the nature of the mode-coupling crossover and show that the strength of the mode-coupling relaxation mechanism depends on the specific model and is very weak in glass-formers with low and intermediate fragility. It would be desirable to understand better why the mode-coupling crossover is more pronounced in harmonic (and presumably hard) spheres than in other models, in order to observe similar qualitative changes in the mechanisms responsible for structural relaxation for other systems and in experimental work. Another issue worth exploring is the idea that using finite sizes may perturb the static structure of the liquid at the level of high-order correlation functions, which in turn could affect the dynamics.

ACKNOWLEDGMENTS

We thank J.-P. Bouchaud for discussions. This work was partly realized with the support of the HPC@LR Center of Competence in High-Performance Computing of Languedoc-Roussillon (France). C.T. acknowledges funding from ERC Advanced Grant No. PTRELSS 228032. G.B. acknowledges funding from ERC Grant No. NPRGGLASS. W.K. acknowledges support from the Institut Universitaire de France.

APPENDIX: MORE RESULTS ON THE KFA MODEL

1. Relaxation time

In this section we discuss the relaxation time of the KFA model, showing the absence of a finite-temperature dynamic singularity for $K < \infty$.

The relaxation mechanism for the square lattice $K = 1$ has been discussed in Ref. [59]. It is explained in terms of the diffusion of macro-vacancies, i.e., extended defects. The relaxation time scale is given by the time it takes for macro-vacancies to diffuse over an area proportional to the inverse of their density. Since the diffusion coefficient of a macro-vacancy simply leads to subleading corrections, one finds that the relaxation time scale is given by the inverse of the probability of having one macro-vacancy around a given site. This reads [59]

$$P = \prod_{\ell=1}^{\infty} [1-(1-c)^{\ell}]^4 \sim e^{-4/c} \sim e^{-4\exp(1/T)} > 0. \quad \text{(A1)}$$

This argument shows that the relaxation time scale cannot be longer than $1/P$, which is a finite number at all T. Therefore, the $K = 1$ model has a relaxation time that only diverges at $T = 0$ and hence has no finite-temperature singularity.

In the opposite limit when $K = \infty$ i.e. on the decorated Bethe lattice the relaxation time scales diverges at a finite T_c and we expect an MCT-like behavior analogous to the one occurring for the pure Bethe lattice where the probability for a site to be unable to relax satisfies the self-consistent relation [58]

$$P = (1-c)[P^3 + 3(1-P)P^2], \quad \text{(A2)}$$

which shows that $P(T \leqslant T_c) = P(T_c) + a\sqrt{T - T_c}$ and corresponds to the well-known "square root" singularity also found in the context of mode-coupling theory [34] and controls for instance the temperature dependence of the long-time limit of the persistence function in the glass phase.

For intermediate K, one can readily generalize the $K = 1$ argument on the probability. The only variant is that instead of requiring one vacancy per side of an expanding square of size ℓ [59], one now requires at least K consecutive up spins on each side of the square. This procedure generates the macro-vacancies of the KFA model. The probability of such a "K macro-vacancy" reads

$$P(K) = c^{K^2} \prod_{\ell=K}^{\infty} [1-(1-c^K)^{\ell/K}]^4 \sim c^{K^2} \exp(-Kc^{-K}) > 0. \quad \text{(A3)}$$

From this argument, we conclude therefore that the KFA model at finite K has no finite-T singularity, as for $K = 1$, but since the above probability $P(K)$ increases rapidly with K, large K values should produce results that are closer to the mean-field Bethe lattice limit obtained at $K = \infty$. The data shown in Fig. 2 are clearly consistent with this expectation, and confirm also that models with larger K have a larger kinetic fragility, i.e., a sharper temperature dependence.

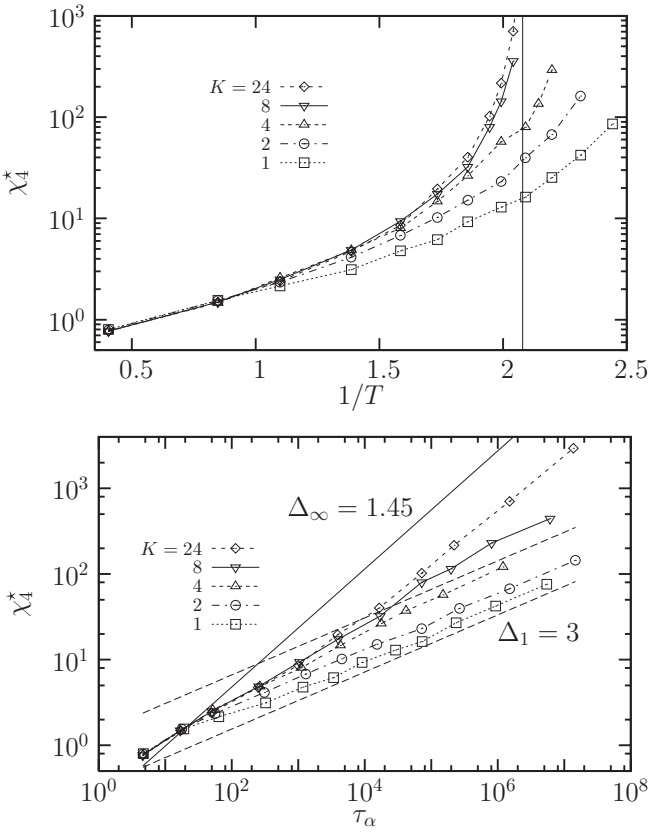

FIG. 10. Top: Temperature evolution of the peak of χ_4 for the KFA model in an Arrhenius plot. Bottom: Dynamic scaling between peak of the susceptibility and relaxation time. Power laws, Eq. (A6), with exponents $\Delta_1 = 3$ and $\Delta_\infty = 1.45$ are shown for comparison.

2. Four-point dynamic susceptibility

In this section we discuss the behavior of the four-point function in the KFA model and in particular its behavior across the mode-coupling crossover.

We define the four-point susceptibility $\chi_4(t)$ in terms of the spontaneous fluctuations of the persistence function [37,64]:

$$\chi_4(t) = N[\langle p^2(t)\rangle - \langle p(t)\rangle^2], \tag{A4}$$

where $p(t)$ is the instantaneous value of the persistence in a system composed of N sites, such that $\langle p(t)\rangle = P(t)$. The time evolution of $\chi_4(t)$ is as found in many other systems. It has a peak whose height $\chi_4^\star$ increases when T decreases, and its position in time shifts to larger times, essentially tracking the alpha-relaxation time. As suggested in previous work [48], the approach to this peak obeys either a single power for $K = 1$ or is composed of two distinct power laws in the mode-coupling regime, $K > 2$.

We follow the temperature evolution of the peak of the dynamic susceptibility, $\chi_4^\star(T)$, in Fig. 10. We use two representations. In Fig. 10(a), we use an Arrhenius plot to emphasize the similarity of behavior of $\chi_4^\star$ with the behavior of $\tau_\alpha(T)$. The crossover nature of these curves is in particular very clear, with a near power-law divergence for $K = 24$, or a much slower growth for $K = 1$. Interestingly, we again find that $\chi_4^\star$ has a mixed behavior for intermediate K values, clearly crossing over from mode-coupling to cooperative behavior near T_c.

This crossover becomes more striking when representing $\chi_4^\star$ as a function of $\tau_\alpha(T)$ using T as a running parameter, as frequently used in studies of glass-forming systems [37,83] [see Fig. 10(b)]. In this representation, both physical regimes are well described by a power-law "dynamic scaling"

$$\chi_4^\star \sim \tau_\alpha^{1/\Delta}, \tag{A5}$$

where the dynamic exponent Δ for a given K takes two values,

$$\Delta(K = \infty) = \Delta_\infty \approx 1.45, \quad \Delta(K = 1) = \Delta_1 \approx 3. \tag{A6}$$

For intermediate K values, the data exhibit a clear crossover from Δ_∞ to Δ_1 as τ_α increases; see for instance the data for $K = 4$ in Fig. 10(b).

It is interesting to note that the mode-coupling crossover, in this simple model at least, is not characterized by a nonmonotonic behavior of $\chi_4(t)$, but rather by a change of its temperature dependence. Although this reflects nicely the change of physical mechanism for structural relaxation near T_c, as shown in Fig. 10, the behavior of χ_4 is not as striking as the nonmonotonic size dependence of $\tau_\alpha(L,T)$ in Fig. 4, and it shows no sign of the nonmonotonic temperature dependence found above for $\ell_{\rm FS}(T)$ or the nonmonotonic dynamic profiles reported near amorphous walls in Ref. [31].

[1] W. Kob, in *Slow Relaxations and Nonequilibrium Dynamics in Condensed Matter*, edited by J.-L. Barrat, J. Dalibard, M. V. Feigel'man, and J. Kurchan (Springer-Verlag, Berlin, 2003).
[2] M. Allen and D. Tildesley, *Computer Simulation of Liquids* (Oxford University Press, Oxford, 1987).
[3] *Finite Size Scaling and Numerical Simulation of Statistical Systems*, edited by V. Privman (World Scientific, Singapore, 1990).
[4] *Dynamical Heterogeneities in Glasses, Colloids, and Granular Media*, edited by L. Berthier, G. Biroli, J.-P. Bouchaud, L. Cipelletti, and W. van Saarloos (Oxford University Press, Oxford, 2011).
[5] P. Ray and K. Binder, Europhys. Lett. **27**, 53 (1994).
[6] C. Donati and J. Jäckle, J. Phys.: Condens. Matter **8**, 2733 (1996).
[7] J. Horbach, W. Kob, K. Binder, and C. A. Angell, Phys. Rev. E **54**, R5897 (1996).
[8] B. Doliwa and A. Heuer, J. Phys.: Condens. Matter **15**, S849 (2003).
[9] S. Büchner and A. Heuer, Phys. Rev. E **60**, 6507 (1999).
[10] K. Kim and R. Yamamoto, Phys. Rev. E **61**, R41 (2000).
[11] J. Jäckle, J. Phys. IV (France) **10**, Pr7-3 (2000).
[12] A. Heuer, J. Phys.: Condens. Matter **20**, 373101 (2008).
[13] L. Berthier, Phys. Rev. Lett. **91**, 055701 (2003).
[14] M. Mosayebi, E. Del Gado, P. Ilg, and H. C. Öttinger, Phys. Rev. Lett. **104**, 205704 (2010).
[15] S. Karmakara, C. Dasgupta, and S. Sastry, Proc. Natl. Acad. Sci. USA **106**, 3675 (2009).
[16] S. Karmakar and I. Procaccia, arXiv:1204.6634.
[17] M. D. Ediger, C. A. Angell, and S. R. Nagel, J. Phys. Chem. **100**, 13200 (1996).
[18] K. Binder and W. Kob, *Glassy Materials and Disordered Solids* (World Scientific, Singapore, 2011).
[19] R. M. Ernst, S. R. Nagel, and G. S. Grest, Phys. Rev. B **43**, 8070 (1991).
[20] J.-L. Barrat and M. L. Klein, Annu. Rev. Phys. Chem. **42**, 23 (1991).
[21] L. Berthier and G. Biroli, Rev. Mod. Phys. **83**, 587 (2011).
[22] J.-P. Bouchaud and G. Biroli, J. Chem. Phys. **121**, 7347 (2004).
[23] A. Montanari and G. Semerjian, J. Stat. Phys. **125**, 22 (2006).
[24] R. L. Jack and J. P. Garrahan, J. Chem. Phys. **123**, 164508 (2005).
[25] A. Cavagna, T. S. Grigera, and P. Verrocchio, Phys. Rev. Lett. **98**, 187801 (2007).
[26] G. Biroli, J.-P. Bouchaud, A. Cavagna, T. S. Grigera, and P. Verrochio, Nat. Phys. **4**, 771 (2008).
[27] G. M. Hocky, T. E. Markland, and D. R. Reichman, Phys. Rev. Lett. **108**, 225506 (2012).
[28] A. Cavagna, T. S. Grigera, and P. Verrocchio, J. Chem. Phys. **136**, 204502 (2012).
[29] R. L. Jack and L. Berthier, Phys. Rev. E **85**, 021120 (2012).
[30] L. Berthier and W. Kob, Phys. Rev. E **85**, 011102 (2012).
[31] W. Kob, S. Roldan-Vargas, and L. Berthier, Nat. Phys. **8**, 164 (2012).
[32] B. Charbonneau, P. Charbonneau, and G. Tarjus, Phys. Rev. Lett. **108**, 035701 (2012).
[33] W. Kob, Sándalo Roldán-Vargas, and L. Berthier, arXiv:1203.4423.
[34] W. Götze, *Complex Dynamics of Glass-Forming Liquids: A Mode-Coupling Theory* (Oxford University Press, Oxford, 2008).

[35] F. Ritort and P. Sollich, Adv. Phys. **52**, 219 (2003).
[36] D. Chandler and J. P. Garrahan, Annu. Rev. Phys. Chem. **61**, 191 (2010).
[37] S. Whitelam, L. Berthier, and J. P. Garrahan, Phys. Rev. Lett. **92**, 185705 (2004); Phys. Rev. E **71**, 026128 (2005).
[38] T. R. Kirkpatrick, D. Thirumalai, and P. G. Wolynes, Phys. Rev. A **40**, 1045 (1989).
[39] G. Biroli and J. P. Bouchaud, arXiv:0912.2542.
[40] S. Franz and A. Montanari, J. Phys. A **40**, F251 (2007).
[41] L. Bocquet and J.-L. Barrat, Europhys. Lett. **31**, 455 (1995).
[42] J. Jäckle and H. Kawai, Physica A **291**, 184 (2001).
[43] F. Martinelli, Lect. Notes Math. **1717**, 93 (2000).
[44] G. Adam and J. H. Gibbs, J. Chem. Phys. **43**, 139 (1965).
[45] D. Kivelson, S. A. Kivelson, X.-L. Zhao, Z. Nussinov, and G. Tarjus, Physica A **219**, 27 (1995).
[46] G. Tarjus, S. A. Kivelson, Z. Nussinov, and P. Viot, J. Phys.: Condens. Matter **17**, R1143 (2005).
[47] X. Y. Xia and P. G. Wolynes, Proc. Natl. Acad. Sci. USA **97**, 2990 (2000).
[48] C. Toninelli, M. Wyart, L. Berthier, G. Biroli, and J.-P. Bouchaud, Phys. Rev. E **71**, 041505 (2005).
[49] G. Biroli and J. P. Bouchaud, Europhys. Lett. **67**, 21 (2004).
[50] L. Berthier and J. P. Garrahan, Phys. Rev. E **68**, 041201 (2003).
[51] S. Franz and G. Semerjian, Chap. 12 in Ref. [4].
[52] C. Brangian, W. Kob, and K. Binder, Europhys. Lett. **53**, 756 (2001).
[53] T. Sarlat, A. Billoire, G. Biroli, and J.-P. Bouchaud, J. Stat. Mech. (2009) P08014.
[54] S. Franz, G. Parisi, F. Ricci-Tersenghi, and T. Rizzo, Eur. Phys. J. E **34**, 102 (2011).
[55] G. H. Fredrickson and H. C. Andersen, Phys. Rev. Lett. **53**, 1244 (1984).
[56] G. H. Fredrickson and H. C. Andersen, J. Chem. Phys. **83**, 5822 (1985).
[57] G. H. Fredrickson and S. A. Brawer, J. Chem. Phys. **84**, 3351 (1986).
[58] M. Sellitto, G. Biroli, and C. Toninelli, Europhys. Lett. **69**, 496 (2005).
[59] C. Toninelli, G. Biroli, and D. S. Fisher, Phys. Rev. Lett. **92**, 185504 (2004).
[60] R. Mari and J. Kurchan, J. Chem. Phys. **135**, 124504 (2011).
[61] M. E. J. Newman and G. T. Barkema, *Monte Carlo Methods in Statistical Physics* (Oxford University Press, Oxford, 1999).
[62] W. Kob and H. C. Andersen, Phys. Rev. E **48**, 4364 (1993).
[63] M. P. Ciamarra, M. Tarzia, A. de Candia, and A. Coniglio, Phys. Rev. E **67**, 057105 (2003).
[64] L. Berthier and J. P. Garrahan, J. Phys. Chem. B **109**, 3578 (2005).
[65] H. Z. Cummins, W. M. Du, M. Fuchs, W. Götze, S. Hildebrand, A. Latz, G. Li, and N. J. Tao, Phys. Rev. E **47**, 4223 (1993).
[66] D. Coslovich and G. Pastore, J. Phys.: Condens. Matter **21**, 285107 (2009).
[67] W. Kob and H. C. Andersen, Phys. Rev. Lett. **73**, 1376 (1994); Phys. Rev. E **51**, 4626 (1995); **52**, 4134 (1995).
[68] H. C. Andersen, Proc. Natl. Acad. Sci. USA **102**, 6686 (2005).
[69] G. Tarjus, D. Kivelson, S. Mossa, and C. Alba-Simionesco, J. Chem. Phys. **120**, 6135 (2004).
[70] B. Bernu, Y. Hitawari, and J.-P. Hansen, J. Phys. **46**, 323 (1985); B. Bernu, J.-P. Hansen, Y. Hiwatari, and G. Pastore, Phys. Rev. A **36**, 4891 (1987).
[71] D. J. Durian, Phys. Rev. Lett. **75**, 4780 (1995).
[72] L. Berthier and T. A. Witten, Europhys. Lett. **86**, 10001 (2009); Phys. Rev. E **80**, 021502 (2009).
[73] J. Horbach and W. Kob, Phys. Rev. B **60**, 3169 (1999).
[74] S. D. Bembenek and B. B. Laird, J. Chem. Phys. **104**, 5199 (1996).
[75] L. Berthier, G. Biroli, J.-P. Bouchaud, W. Kob, K. Miyazaki, and D. Reichman, J. Chem. Phys. **126**, 184504 (2007); **126**, 184503 (2007).
[76] A. Saksaengwijit and A. Heuer, Phys. Rev. E **73**, 061503 (2006).
[77] M. Vogel and S. C. Glotzer, Phys. Rev. Lett. **92**, 255901 (2004); Phys. Rev. E **70**, 061504 (2004).
[78] L. Berthier, Phys. Rev. E **76**, 011507 (2007).
[79] C. Donati, S. C. Glotzer, and P. H. Poole, Phys. Rev. Lett. **82**, 5064 (1999).
[80] C. Donati, S. C. Glotzer, P. H. Poole, W. Kob, and S. J. Plimpton, Phys. Rev. E **60**, 3107 (1999).
[81] L. Berthier, Phys. Rev. E **69**, 020201(R) (2004).
[82] S. Karmakar, C. Dasgupta, and S. Sastry, Phys. Rev. Lett. **105**, 015701 (2010).
[83] C. Dalle-Ferrier, C. Thibierge, C. Alba-Simionesco, L. Berthier, G. Biroli, J.-P. Bouchaud, F. Ladieu, D. L'Hôte, and G. Tarjus, Phys. Rev. E **76**, 041510 (2007).
[84] S. Karmakar (private communication).
[85] D. Coslovich and G. Pastore, J. Chem. Phys. **127**, 124504 (2007).
[86] D. Coslovich, Phys. Rev. E **83**, 051505 (2011).
[87] J.-N. Roux, J.-L. Barrat, and J.-P. Hansen, J. Phys.: Condens. Matter **1**, 7171 (1989).
[88] R. Yamamoto and A. Onuki, Phys. Rev. Lett. **81**, 4915 (1998).
[89] U. R. Pedersen, T. B. Schroder, J. C. Dyre, and P. Harrowell, Phys. Rev. Lett. **104**, 105701 (2010).
[90] T. S. Grigera, A. Cavagna, I. Giardina, and G. Parisi, Phys. Rev. Lett. **88**, 055502 (2002).
[91] L. Berthier and W. Kob, J. Phys.: Condens. Matter **19**, 205130 (2007).